


RESEARCH ARTICLE

Adaptive-observer-based robust control for a time-delayed teleoperation system with scaled four-channel architecture

Liping Chan* , Qingqing Huang and Ping Wang

Automation College, Chongqing University of Posts and Telecommunications, Chongqing, 400065, China

*Corresponding author. E-mail: lc842@uowmail.edu.au

Received: 17 December 2020; **Revised:** 27 June 2021; **Accepted:** 27 July 2021; **First published online:** 3 September 2021

Keywords: Bilateral teleoperation; Scaled 4-CH teleoperation; Improved extended active observer; Damping injection; Model uncertainty; Time-varying delay

Abstract

This article presents an innovative adaptive-observer-based scaled four-channel (4-CH) control approach applying damping injection for nonlinear teleoperation systems, which unify the study of robotic dynamic uncertainties, operator/environment force requirements and asymmetric time-varying delays in the same framework. First, a scaled 4-CH scheme with damping injection is developed to handle time-varying delay while guaranteeing the passivity of communication channels. Then, the improved extended active observer (IEAOB) is deployed to derive the operator/environment force while addressing the issues of measurement noise and model uncertainties. Furthermore, the system stability is analyzed by choosing Lyapunov functional. Finally, the proposed method is validated through simulation.

1. Introduction

Due to the capabilities of extending human sensing, decision making and manipulation to the remote object by the exchange of various information, the bilateral teleoperation system has attracted much attention over the past decades and become a very hot and challenging topic of control technologies with numerous applications, such as space operation, underwater exploration and mining, handling toxic or nuclear materials, as well as, robotic-assisted surgical interventions [1]. There are two major control objectives in a bilateral teleoperation system: stability and transparency. The system stability would be easily affected by the nonzero communication time delay, which causes performance degradation and, in the worst scenario, instability of the overall system. Transparency indicates that the technical medium between operator and environment is not felt, that is, the dynamics of master and slave are canceled out [2]. Since force feedback may cause instability, enhancing transparency and simultaneously guaranteeing stability is a challenge in bilateral teleoperation systems [3]. To fight against the time delay in a teleoperation system, various control strategies [4, 5] have been reported in the literature. Prevalent among these approaches is the passivity-based control method, which makes the use of scattering transformations for constant time delays [6] and variable time delays in [7, 8]. However, as the time delay increases, these scattering-based methods would cause wave reflection and position drift, and accordingly the practicality of the teleoperation system decreases due to the reduced transparency. Hence, many modifications [9, 10, 11, 12] have been proposed for the wave-variable-based approaches to reinforce the system performance. As one of the other passivity-based control schemes, damping injection controllers, which deploy delayed position and velocity error terms (PD) in addition to the delayed proportional term (d), can provide good position tracking performance in the presence of constant [13] or variable time delays [14, 15]. Readers can refer to [16] for an extensive survey of various bilateral teleoperation control approaches, and [17] for a recent survey of passivity-based approaches. As more complex teleoperation tasks are increasing in recent years, the nonlinearity and uncertainty, essentially

existing in robot manipulators have become another formidable barrier to achieve a high level of fidelity while maintaining system stability. Many control schemes have been reported in the engineering community to deal with these problems, such as adaptive control [18, 19, 20, 21, 22, 23, 24], robust control [25, 26, 27, 28, 29, 30], and neural network and fuzzy logic technique [31, 32, 33, 34, 35, 36, 37], etc.

In addition, the literature reveals that very few methods apply direct force signals reflection in the nonlinear teleoperation system under time delays, although the force reflection can greatly enforce the realistic haptic perception felt by the operators and increase the system transparency. The reason is that the design of the force source and the transmission of the external force signals in delayed communication channels may adversely affect the passivity of the communication channels and jeopardize the stability of the teleoperation system using the passivity-based controllers [38]. Therefore, designing control strategies to accurately derive external force signals and transmit command signals without jeopardizing the system stability is a big challenge for bilateral teleoperation. Four-channel teleoperation architecture, proposed in [39] and [40] to realize ideal transparency, can achieve the perfect position tracking between master and slave robots and perfect force reflection from the environment to the operator by transmitting the force and position information from both robots. In some micromanipulation applications, such as tele-surgery, as the master and the slave works on the macroscale and microscale, respectively, the scaled four-channel control is required, which means the master position and human force information are scaled down to the slave while the slave position and environment force information are scaled up to the master. Since the four-channel teleoperation architecture is known to provide the best performance in terms of transparency [41], the combination of the (scaled) four-channel and passivity-based approaches could be an effective way to achieve stability and good transparency performance simultaneously for a nonlinear bilateral teleoperation system in the presence of constant or time-varying delays [42, 43].

Motivated by the aforementioned discussions, a novel adaptive-observer-based scaled four-channel (4-CH) control approach applying damping injection for nonlinear teleoperation systems is developed in this article to achieve very good synchronization between the master and slave robots whether the slave robot is during free motion or in contact with the environment. The investigated design can cope with the majority of the control issues in a nonlinear teleoperation system, such as robot dynamical model uncertainties, external noises, external operator and environment force requirements and time-varying delays. The stability of the proposed teleoperation system is guaranteed in the presence of bounded disturbances and time-varying delays. The effectiveness of the system is demonstrated through simulation. Specifically, the work offers the following contributions:

1. A novel scaled 4-CH control scheme with the damping injection is developed to handle time-varying delays and improve the position and force tracking performance in addition to guaranteeing the passivity of the communication channels and accordingly the stability of the whole system.
2. The improved extended active observers (IEAOBs) are employed at both the master and slave sides to accurately estimate the external operator/environment forces and velocity signals while simultaneously eliminating the external noise and coping with the robot parameter variation issues.
3. By building a proper Lyapunov–Krasovskii functional, the close-loop master–slave teleoperation system stability and performance under time-varying delays is analyzed.
4. The theoretical work presented here is supported by simulation results based on a 2-DOF master–slave teleoperation system.

The remainder of the article is structured as follows: after stating the model of the nonlinear teleoperation system and the control objective in Section 2, the proposed scaled 4-CH control scheme applying damping injection will be described in Section 3. In this section, the stability analysis will be also discussed. In Section 4, simulation results are provided followed by the conclusion in Section 5.

2. Problem formulation

The dynamics of the nonlinear teleoperation system consisting of a pair of n-degree-of-freedom (DOF) robots with revolute joints can be formulated as:

$$M_m(q_m, \theta_m) \ddot{q}_m + V_m(q_m, \dot{q}_m, \theta_m) \dot{q}_m + g_m(q_m, \theta_m) + T_{f_m} = T_m + T_h, \tag{1a}$$

$$M_s(q_s, \theta_s) \ddot{q}_s + V_s(q_s, \dot{q}_s, \theta_s) \dot{q}_s + g_s(q_s, \theta_s) + T_{f_s} = T_s + T_e, \tag{1b}$$

where $\ddot{q}_*, \dot{q}_*, q_*$ ($*$ = m/s) are angular acceleration, angular velocity and angular position signals, $M_*(q_*, \theta_*)$ is the inertia matrix, $V_*(q_*, \dot{q}_*, \theta_*)$ is the vector of Coriolis and centripetal terms, $g_*(q_*, \theta_*)$ is the gravity torque, T_{f_*} are the friction torques, T_* are input torques of the controllers, θ_* represent inertial robotic parameters and T_h, T_e correspond to the torques exerted by the human operator and environment, respectively. In this study, T_{f_*} is modeled as a simplified version of the LuGre model [44], by considering viscous and Coulomb friction:

$$T_{f_*} = v_{c_*} * \text{sgn}(\dot{q}_*) + v_{v_*} * \dot{q}_*, \tag{2}$$

where $v_{c_*} \in R^n$ is the coefficient vector of Coulomb friction, and $v_{v_*} \in R^n$ is the coefficient vector of viscous friction.

When one treats the external human or environment force acting on a manipulator as an unknown input and models it as a random walk process, and also considers that the master and slave robot dynamics are nonlinear with parameter variations, by defining the state vector X_* ($*$ = m/s) as $X_* = [q_* \ \dot{q}_* \ \theta_* \ v_{v_*} \ v_{c_*} \ T_{h/e}]^T$, the teleoperation system model in (1) can be extended in state-space representation as follows:

$$\dot{X}_* = f_*(X_*, T_*) + G_* \xi_{X_*} = \begin{bmatrix} \dot{q}_* \\ M_*^{-1}(-V_*\dot{q}_* - g_* - T_{f_*} + T_* + T_{h/e}) \\ 0 \\ 0 \\ 0 \\ 0 \end{bmatrix} + G_* \begin{bmatrix} \xi_{q_*} \\ \xi_{\dot{q}_*} \\ \xi_{\theta_*} \\ \xi_{v_{v_*}} \\ \xi_{v_{c_*}} \\ \xi_{T_{h/e}} \end{bmatrix}, \tag{3a}$$

$$Y_* = H_* X_* + \eta_{X_*} = [I \ 0 \ 0 \ 0 \ 0 \ 0] \begin{bmatrix} q_* \\ \dot{q}_* \\ \theta_* \\ v_{v_*} \\ v_{c_*} \\ T_{h/e} \end{bmatrix} + \eta_{X_*}, \tag{3b}$$

where Y_* is the output of the system, G_* is a unit matrix and the state observation matrix $H_* = [I \ 0 \ 0 \ 0 \ 0 \ 0]$, and $\xi_{q_*}, \xi_{\dot{q}_*}$ and η_{X_*} represent the process noises and measurement noises, respectively, $\xi_{T_{h/e}}, \xi_{v_{v_*}}, \xi_{v_{c_*}}$ and ξ_{θ_*} represent the rates at which the vectors of external torques, friction coefficients and robot parameters are estimated to vary.

Some important properties of the above nonlinear robot dynamic model, which will be used in the analysis of the teleoperation system, can be obtained as follows [37]:

Property 1. The inertia matrix $M_*(q_*)$ for a manipulator is symmetric positive-definite which verifies:

$$0 < \sigma_{\min}(M_*(q_*)) I \leq M_*(q_*) \leq \sigma_{\max}(M_*(q_*)) I < \infty, \tag{4}$$

where $I \in R^{n \times n}$ is the identity matrix. σ_{\min} and σ_{\max} denote the strictly positive minimum and maximum eigenvalue of M_* for all configurations q_* ($* = m/s$).

Property 2. Under an appropriate definition of the Coriolis/centrifugal matrix, the matrix $\dot{M}_* - 2V_*$ is skew symmetric, which can also be expressed as:

$$\dot{M}_*(q_*(t)) = V_*(q_*(t), \dot{q}_*(t)) + V_*^T(q_*(t), \dot{q}_*(t)). \tag{5}$$

In addition, some assumptions for this work are stated as

Assumption 1. It is assumed that there are time-varying delays in the forward and feedback communication channel. $t(t) = T_1(t) + T_2(t)$ represents the round-trip time delay, $T_1(t)$ is the forward communication channel-induced delay, $T_2(t)$ is the feedback communication channel-induced delay. The variable time-delays $T_*(t)$ and the derivatives $\dot{T}_*(t)$ have known upper bounds, i.e., $0 \leq T_*(t) \leq T_{*max} < \infty$, $* = 1, 2$. It is reasonable to assume that the time-varying delay in the communication channel is bounded from a practical point of view. Infinite time delays imply that the connection between the master side and the slave side is broken. Furthermore, the variable time-delays do not increase or decrease faster than time itself [11, 13, 14, 17], i.e., $|\dot{T}_*(t)| < 1$, $* = 1, 2$.

Assumption 2. we assume that the operational and environmental torques are passive and satisfy:

$$-\int_0^t \dot{q}_m^T(\eta) T_h(\eta) d\eta + \rho_h \geq 0, \tag{6}$$

and

$$-\int_0^t \dot{q}_s^T(\eta) T_e(\eta) d\eta + \rho_e \geq 0, \tag{7}$$

for $\exists \rho_h, \rho_e > 0, \forall t \geq 0$. For the system stability analysis later, the operational and environmental torques are modeled as [11]

$$T_h(t) = -\varnothing_m(\dot{q}_m(t) + \rho q_m(t)), \tag{8a}$$

$$T_e(t) = \varnothing_s(\dot{q}_s(t) + \rho q_s(t)), \tag{8b}$$

where ρ , \varnothing_m and \varnothing_s are positive constant and matrices and are properties of the human and the environment, respectively.

The control objective is to achieve asymptotic master–slave coordination in free motion and asymptotic force reflection in the steady state in the presence of time-varying delays and bounded parameter variations and external disturbances. To accomplish that, we will present the proposed adaptive-observer-based scaled four-channel (4-CH) control approach with damping injection in the following section with three steps:

- Step 1:* Design the novel adaptive scaled 4-CH control scheme with the damping injection to compensate the effect of the time-varying delay and improve position and force tracking performance.
- Step 2:* Design the IEAOB at both master and slave sides to identify the nonlinear robot dynamical model and estimate the external forces, position and velocity signals in the presence of measurement noises.
- Step 3:* Build proper Lyapunov–Krasovskii functional to analyse the overall system stability and find sufficient conditions on the controller parameters to guarantee the system performance.

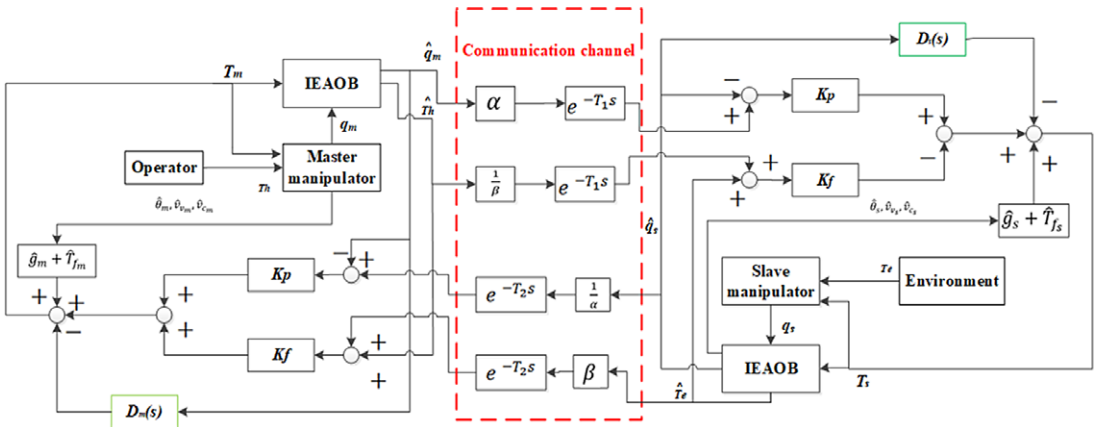


Figure 1. The proposed scaled 4-CH control architecture for bilateral teleoperation manipulators.

3. Adaptive-observer-based robust control approach with scaled 4-CH architecture

In this section, the adaptive scaled 4-CH method with damping injection is developed to handle the time-varying delay first. Then, the IEAOBs are deployed at both master and slave sides to identify the robot model and estimate the external force while dealing with dynamic uncertainties and external noises. After that, the stability of the proposed bilateral control system is theoretically analyzed.

3.1. The proposed scaled 4-CH teleoperation architecture with damping injection

Figure 1 shows the proposed control architecture for a nonlinear time-delayed bilateral teleoperation system. The master position and human force signals $\hat{q}_m(t)$, \hat{T}_h are scaled by α and $1/\beta$, respectively, and then transmitted to the slave through the forward communication channel e^{-T_1s} , and the IEAOB is designed at the slave side to estimate the robot model parameters $(\hat{\theta}_s, \hat{v}_{cs}, \hat{v}_{vs})$ and environment torque \hat{T}_e . The estimated robot parameters $(\hat{\theta}_s, \hat{v}_{cs}, \hat{v}_{vs})$ are utilized to calculate the estimated \hat{g}_s and \hat{T}_{fs} for compensation of the gravity item and friction, and the slave controller T_s based on the estimated torque \hat{g}_s and \hat{T}_{fs} , the force controller K_f , the position controller K_p , and damping injection $D_s(s)$ is designed for the slave manipulator to achieve great tracking position performance under various noises and uncertainties. The slave position signal $\hat{q}_s(t)$ and the estimated environment torque \hat{T}_e are scaled by $1/\alpha$ and β , respectively, and then transmitted to the master via the feedback communication channel e^{-T_2s} to design the controller at the master side. The IEAOB is designed at the master side as well for the master robot to identify the dynamical model $(\hat{\theta}_m, \hat{v}_{cm}, \hat{v}_{vm})$ and estimate the human operator torque \hat{T}_h , which are then used in the master controller design under various noises and uncertainties. Similar to the slave side, the estimated robot parameters $(\hat{\theta}_m, \hat{v}_{cm}, \hat{v}_{vm})$ are utilized to calculate the estimated \hat{g}_m and \hat{T}_{fm} for compensation of the gravity item and friction, and the master controller T_m is built based on the estimated torque \hat{g}_m and \hat{T}_{fm} , the force controller K_f , the position controller K_p , and damping injection $D_m(s)$. The master control design is simplified to let the forces track as closely as possible. Therefore, good transparency performance can be obtained with the satisfied position tracking performance for the slave robot and the actual feeling of estimated environmental torque provided for the human operator.

Let's define $e_{mp} = \frac{1}{\alpha}q_s(t - T_2(t)) - q_m(t)$, $e_{sp} = \alpha q_m(t - T_1(t)) - q_s(t)$, $e_{mf} = \beta T_e(t - T_2(t)) + T_h$, $e_{sf} = T_e + \frac{1}{\beta}T_h(t - T_1(t))$, the proposed controllers for master and slave robots are:

$$T_m = \bar{T}_m + \hat{T}_{fm} + \hat{g}_m(\hat{q}_m, \hat{\theta}_m) - D_m(s) * \hat{q}_m; \tag{9a}$$

$$T_s = \bar{T}_s + \hat{T}_{fs} + \hat{g}_s(\hat{q}_s, \hat{\theta}_s) - D_s(s) * \hat{q}_s; \tag{9b}$$

where

$$\bar{T}_m = K_p \widehat{e}_{mp} + K_f \widehat{e}_{mf}, \tag{10a}$$

$$\bar{T}_s = K_p \widehat{e}_{sp} - K_f \widehat{e}_{sf}, \tag{10b}$$

where α, β are the position and force scaling factors, respectively, K_f, K_p are the force controller and position controller, respectively, the damping coefficients $D_m(s) = K_{bm}s, D_s(s) = K_{bs}s, \widehat{*}$ is the estimate item by the IEAOB, which will be presented in the following subsection.

3.2. IEAOB for master/slave model identification and external force estimation

Due to the nonlinearity and uncertainty essentially existing in robot manipulators, it is very difficult to achieve a high level of fidelity while maintaining system stability for a bilateral teleoperation system if the issue is not well addressed. Therefore, in this subsection, the IEAOB in [19] is employed to identify the accurate nonlinear robot model as well as estimate the external force without knowing a specific external force model in the presence of friction, processing noise and measurement noise. Let’s recall the dynamical model for master and slave robots in (3), the IEAOB is designed as follows:

$$\dot{\widehat{X}}_* = f_*(\widehat{X}_*, T_*) + P_* H_*^T R_*^{-1} (Y_* - H_* \widehat{X}_*), \tag{11a}$$

where

$$\dot{P}_* = \frac{\partial f_*}{\partial \widehat{X}_*} P_* + P_* \frac{\partial f_*^T}{\partial \widehat{X}_*} + G_* Q_* G_*^T - P_* H_*^T R_*^{-1} H_* P_*, \tag{11b}$$

and

$$R_* = \text{cov}(\eta_{X_*}),$$

$$Q_* = \text{diag}(\text{cov}(\xi_{q_*}), \text{cov}(\xi_{\dot{q}_*}), \text{cov}(\xi_{\theta_*}), \text{cov}(\xi_{v_{v_*}}), \text{cov}(\xi_{v_{c_*}}), \text{cov}({}^0\xi_{T_{h/e}})),$$

$$f_*(\widehat{X}_*, T_*) = \begin{bmatrix} f_{*1} \\ f_{*2} \\ f_{*3} \\ f_{*4} \\ f_{*5} \\ f_{*6} \end{bmatrix} = \begin{bmatrix} \dot{\widehat{q}}_* \\ \ddot{\widehat{q}}_* \\ \widehat{\theta}_* \\ \widehat{v}_{v_*} \\ \widehat{v}_{c_*} \\ \widehat{T}_{h/e} \end{bmatrix} = \begin{bmatrix} \widehat{q}_* \\ \widehat{M}_*^{-1}(-\widehat{V}_* \widehat{q}_* - \widehat{g}_* + T_* + \widehat{T}_{h/e} - \widehat{T}_{f_*}) \\ 0 \\ 0 \\ 0 \\ 0 \end{bmatrix}, \tag{12a}$$

where $f_{*1} = \dot{\widehat{q}}_*, f_{*2} = \widehat{M}_*^{-1}(-\widehat{V}_* \widehat{q}_* - \widehat{g}_* + T_* + \widehat{T}_{h/e} - \widehat{T}_{f_*}), f_{*3} = 0, f_{*4} = 0, f_{*5} = 0, f_{*6} = 0, * = m/s, \text{cov}(\xi_{q_*}), \text{cov}(\xi_{\dot{q}_*}), \text{cov}(\xi_{\theta_*}), \text{cov}(\xi_{v_{v_*}}), \text{cov}(\xi_{v_{c_*}}), \text{cov}({}^0\xi_{T_{h/e}})$, and $\text{cov}(\eta_{X_*})$ are, respectively, the covariance matrices of the input stochastic, zero mean, and Gaussian noises $\xi_{q_*}, \xi_{\dot{q}_*}, \xi_{\theta_*}, \xi_{v_{v_*}}, \xi_{v_{c_*}}, {}^0\xi_{T_{h/e}}$, and the output stochastic, zero mean, and Gaussian noise η_{X_*} , and

$$F_*(t) = \frac{\partial f_*}{\partial \widehat{X}_*} = \begin{bmatrix} \frac{\partial f_{*1}}{\partial \widehat{q}_*} & \frac{\partial f_{*1}}{\partial \dot{\widehat{q}}_*} & \frac{\partial f_{*1}}{\partial \theta_*} & \frac{\partial f_{*1}}{\partial v_{v_*}} & \frac{\partial f_{*1}}{\partial v_{c_*}} & \frac{\partial f_{*1}}{\partial T_{h/e}} \\ \frac{\partial f_{*2}}{\partial \widehat{q}_*} & \frac{\partial f_{*2}}{\partial \dot{\widehat{q}}_*} & \frac{\partial f_{*2}}{\partial \theta_*} & \frac{\partial f_{*2}}{\partial v_{v_*}} & \frac{\partial f_{*2}}{\partial v_{c_*}} & \frac{\partial f_{*2}}{\partial T_{h/e}} \\ \frac{\partial f_{*3}}{\partial \widehat{q}_*} & \frac{\partial f_{*3}}{\partial \dot{\widehat{q}}_*} & \frac{\partial f_{*3}}{\partial \theta_*} & \frac{\partial f_{*3}}{\partial v_{v_*}} & \frac{\partial f_{*3}}{\partial v_{c_*}} & \frac{\partial f_{*3}}{\partial T_{h/e}} \\ \frac{\partial f_{*4}}{\partial \widehat{q}_*} & \frac{\partial f_{*4}}{\partial \dot{\widehat{q}}_*} & \frac{\partial f_{*4}}{\partial \theta_*} & \frac{\partial f_{*4}}{\partial v_{v_*}} & \frac{\partial f_{*4}}{\partial v_{c_*}} & \frac{\partial f_{*4}}{\partial T_{h/e}} \\ \frac{\partial f_{*5}}{\partial \widehat{q}_*} & \frac{\partial f_{*5}}{\partial \dot{\widehat{q}}_*} & \frac{\partial f_{*5}}{\partial \theta_*} & \frac{\partial f_{*5}}{\partial v_{v_*}} & \frac{\partial f_{*5}}{\partial v_{c_*}} & \frac{\partial f_{*5}}{\partial T_{h/e}} \\ \frac{\partial f_{*6}}{\partial \widehat{q}_*} & \frac{\partial f_{*6}}{\partial \dot{\widehat{q}}_*} & \frac{\partial f_{*6}}{\partial \theta_*} & \frac{\partial f_{*6}}{\partial v_{v_*}} & \frac{\partial f_{*6}}{\partial v_{c_*}} & \frac{\partial f_{*6}}{\partial T_{h/e}} \end{bmatrix}$$

$$= \begin{bmatrix} 0 & I & 0 & 0 & 0 & 0 \\ F_{*21}(t) & F_{*22}(t) & F_{*23}(t) & F_{*24}(t) & F_{*25}(t) & F_{*26}(t) \\ 0 & 0 & 0 & 0 & 0 & 0 \\ 0 & 0 & 0 & 0 & 0 & 0 \\ 0 & 0 & 0 & 0 & 0 & 0 \\ 0 & 0 & 0 & 0 & 0 & 0 \end{bmatrix}. \tag{12b}$$

Now we will show how to get $F_{*21}(t), F_{*22}(t), F_{*23}(t), F_{*24}(t), F_{*25}(t), F_{*26}(t)$ in (12b).

Let's first consider

$$\frac{\partial(\widehat{M}_* * \widehat{M}_*^{-1})}{\partial \widehat{q}_*} = \frac{\partial I}{\partial \widehat{q}_*} = 0 = \frac{\partial \widehat{M}_*}{\partial \widehat{q}_*} * \widehat{M}_*^{-1} + \widehat{M}_* * \frac{\partial \widehat{M}_*^{-1}}{\partial \widehat{q}_*},$$

Then, we can get

$$\frac{\partial \widehat{M}_*^{-1}}{\partial \widehat{q}_*} = -\widehat{M}_*^{-1} * \frac{\partial \widehat{M}_*}{\partial \widehat{q}_*} * \widehat{M}_*^{-1}.$$

Similarly, one can have

$$\frac{\partial \widehat{M}_*^{-1}}{\partial \widehat{\theta}_*} = -\widehat{M}_*^{-1} * \frac{\partial \widehat{M}_*}{\partial \widehat{\theta}_*} * \widehat{M}_*^{-1}.$$

Hence,

$$\begin{aligned} F_{*21}(t) &= \frac{\partial f_{*2}}{\partial \widehat{q}_*} = -\widehat{M}_*^{-1} * \frac{\partial \widehat{M}_*}{\partial \widehat{q}_*} * \widehat{M}_*^{-1} * (-\widehat{V}_* \widehat{q}_* - \widehat{g}_* + T_* + \widehat{T}_{h/e} - \widehat{T}_{f_*}) \\ &\quad - \widehat{M}_*^{-1} * \left(\frac{\partial \widehat{V}_* \widehat{q}_*}{\partial \widehat{q}_*} + \frac{\partial \widehat{g}_*}{\partial \widehat{q}_*} + \frac{\partial \widehat{T}_{f_*}}{\partial \widehat{q}_*} \right) = -\widehat{M}_*^{-1} \left(\frac{\partial \widehat{M}_*}{\partial \widehat{q}_*} \widehat{q}_* + \frac{\partial \widehat{V}_* \widehat{q}_*}{\partial \widehat{q}_*} + \frac{\partial \widehat{g}_*}{\partial \widehat{q}_*} + \frac{\partial \widehat{T}_{f_*}}{\partial \widehat{q}_*} \right), \\ F_{*22}(t) &= \frac{\partial f_{*2}}{\partial \widehat{q}_*} = -\widehat{M}_*^{-1} \left(\frac{\partial \widehat{V}_* \widehat{q}_*}{\partial \widehat{q}_*} + \frac{\partial \widehat{T}_{f_*}}{\partial \widehat{q}_*} \right), \\ F_{*23}(t) &= \frac{\partial f_{*2}}{\partial \widehat{\theta}_*} = -\widehat{M}_*^{-1} * \frac{\partial \widehat{M}_*}{\partial \widehat{\theta}_*} * \widehat{M}_*^{-1} * (-\widehat{V}_* \widehat{q}_* - \widehat{g}_* + T_* + \widehat{T}_{h/e} - \widehat{T}_{f_*}) \\ &\quad - \widehat{M}_*^{-1} * \left(\frac{\partial \widehat{V}_* \widehat{q}_*}{\partial \widehat{\theta}_*} + \frac{\partial \widehat{g}_*}{\partial \widehat{\theta}_*} \right) = -\widehat{M}_*^{-1} \left(\frac{\partial \widehat{M}_*}{\partial \widehat{\theta}_*} \widehat{q}_* + \frac{\partial \widehat{V}_* \widehat{q}_*}{\partial \widehat{\theta}_*} + \frac{\partial \widehat{g}_*}{\partial \widehat{\theta}_*} \right), \\ F_{*24}(t) &= \frac{\partial f_{*2}}{\partial \widehat{v}_{c_*}} = -\widehat{M}_*^{-1} \frac{\partial \widehat{T}_{f_*}}{\partial \widehat{v}_{c_*}}, F_{*25}(t) = \frac{\partial f_{*2}}{\partial \widehat{v}_{c_*}} = -\widehat{M}_*^{-1} \frac{\partial \widehat{T}_{f_*}}{\partial \widehat{v}_{c_*}}, F_{*26}(t) = \frac{\partial f_{*2}}{\partial \widehat{T}_{h/e}} = \widehat{M}_*^{-1}. \end{aligned}$$

Then, one has

$$\widehat{T}_{f_*} = \widehat{v}_{c_*} \operatorname{sgn}(\widehat{q}_*) + \widehat{v}_{v_*} \widehat{q}_*. \tag{13}$$

It is worth stressing that the implementation of the IEAOB into real-world applications would not be easy due to the massive calculation of the inverse of inertia matrix \widehat{M}_*^{-1} . However, Bierman et al. [45] provide one way to optimize the derivation of the IEAOB, and the calculation is largely reduced according to the result in [45].

3.3. Stability analysis

In this subsection, the stability for the nonlinear bilateral teleoperation system with the proposed control law is analyzed.

Theorem 1. In the nonlinear teleoperation system described by equation (1) with the control law in (9-10), the external force modelled as (8) and the IEAOB in (11), the velocities \dot{q}_m, \dot{q}_s and position error e_{mp}, e_{sp} are bounded ($\dot{q}_m, \dot{q}_s, e_{mp}, e_{sp} \in L_2 \cap L_\infty$), provided that

$$1) \quad K_{bm} + \frac{1}{2}K_p A_1 - \frac{1}{1 - \dot{T}_1(t)} \frac{1}{2} \frac{B_1}{B_2} K_p A_2 - \frac{K_p B_1}{2} \left(\omega_1 + \frac{T_{1max}^2}{\omega_2} \right) > 0,$$

$$2) \quad K_{bs} + \frac{1}{2} \frac{B_1}{B_2} K_p A_2 - \frac{1}{1 - \dot{T}_2(t)} \frac{1}{2} K_p A_1 - \frac{K_p B_1}{2} \left(\omega_2 + \frac{T_{2max}^2}{\omega_1} \right) > 0,$$

$$3) \quad \alpha_1 I \leq Q_m(t) \leq \alpha_2 I, \beta_1 I \leq Q_s(t) \leq \beta_2 I,$$

$$4) \quad \alpha_3 I \leq R_m(t) \leq \alpha_4 I, \beta_3 I \leq R_s(t) \leq \beta_4 I,$$

5) The following is true:

$$\alpha_5 I \leq \int_t^{t+\sigma} \begin{bmatrix} F_{m23}(\tau) & F_{m24}(\tau) & F_{m25}(\tau) & F_{m26}(\tau) \end{bmatrix}^T * \\ \begin{bmatrix} F_{m23}(\tau) & F_{m24}(\tau) & F_{m25}(\tau) & F_{m26}(\tau) \end{bmatrix} d\tau \leq \alpha_6 I,$$

where $F_{m23}(\tau), F_{m24}(\tau), F_{m25}(\tau)$ and $F_{m26}(\tau)$ are evaluated along \widehat{X}_m and $\dot{F}_{m23}(\tau), \dot{F}_{m24}(\tau), \dot{F}_{m25}(\tau)$ and $\dot{F}_{m26}(\tau)$ are bounded, with

$$F_{m23}(t) = -\widehat{M}_m^{-1} \left(\frac{\partial \widehat{M}_m}{\partial \widehat{\theta}_m} \dot{\widehat{q}}_m + \frac{\partial \widehat{V}_m}{\partial \widehat{\theta}_m} \widehat{q}_m + \frac{\partial \widehat{g}_m}{\partial \widehat{\theta}_m} \right),$$

$$F_{m24}(t) = -\widehat{M}_m^{-1} \frac{\partial \widehat{T}_{f_m}}{\partial \widehat{v}_{v_m}},$$

$$F_{m25}(t) = -\widehat{M}_m^{-1} \frac{\partial \widehat{T}_{f_m}}{\partial \widehat{v}_{c_m}},$$

$$F_{m26}(t) = \widehat{M}_m^{-1},$$

for some positive constants $\alpha_1, \alpha_2, \alpha_3, \alpha_4, \alpha_5, \alpha_6, \sigma$ and all $t > t_0$,

6) The following is true:

$$\beta_5 I \leq \int_t^{t+\sigma} \begin{bmatrix} F_{s23}(\tau) & F_{s24}(\tau) & F_{s25}(\tau) & F_{s26}(\tau) \end{bmatrix}^T * \\ \begin{bmatrix} F_{s23}(\tau) & F_{s24}(\tau) & F_{s25}(\tau) & F_{s26}(\tau) \end{bmatrix} d\tau \leq \beta_6 I,$$

where $F_{s23}(\tau)$, $F_{s24}(\tau)$, $F_{s25}(\tau)$ and $F_{s26}(\tau)$ are evaluated along \widehat{X}_s and $\dot{F}_{s23}(\tau)$, $\dot{F}_{s24}(\tau)$, $\dot{F}_{s25}(\tau)$ and $\dot{F}_{s26}(\tau)$ are bounded, with

$$\begin{aligned}
 F_{s23}(t) &= -\widehat{M}_s^{-1} \left(\frac{\partial \widehat{M}_s}{\partial \widehat{\theta}_s} \dot{\widehat{q}}_s + \frac{\partial \widehat{V}_s \widehat{q}_s}{\partial \widehat{\theta}_s} + \frac{\partial \widehat{g}_s}{\partial \widehat{\theta}_s} \right), \\
 F_{s24}(t) &= -\widehat{M}_s^{-1} \frac{\partial \widehat{T}_{fs}}{\partial \widehat{V}_{vs}}, \\
 F_{s25}(t) &= -\widehat{M}_s^{-1} \frac{\partial \widehat{T}_{fs}}{\partial \widehat{V}_{cs}}, \\
 F_{s26}(t) &= \widehat{M}_s^{-1},
 \end{aligned}$$

for some positive constants $\beta_1, \beta_2, \beta_3, \beta_4, \beta_5, \beta_6, \sigma$ and all $t > t_0$.

Proof: Define $\ddot{q}_* = \ddot{q}_* - \ddot{\widehat{q}}_*$, $\dot{q}_* = \dot{q}_* - \dot{\widehat{q}}_*$, $\widehat{q}_* = q_* - \widehat{q}_*$, $\widetilde{\theta}_* = \theta_* - \widehat{\theta}_*$, $\widetilde{T}_{h/e} = T_{h/e} - \widehat{T}_{h/e}$, where $* = m/s$. If conditions 3,4,5,6 of the Theorem and Property 1 in Section 2 are satisfied, according to Theorem 1 in [19], the estimated signals converge to real values asymptotically, then we have

$$\lim_{t \rightarrow \infty} |\widetilde{q}_*| = 0, \lim_{t \rightarrow \infty} |\dot{\widetilde{q}}_*| = 0, \lim_{t \rightarrow \infty} |\widetilde{\theta}_m| = 0, \lim_{t \rightarrow \infty} |\widetilde{T}_h| = 0, \lim_{t \rightarrow \infty} |\widetilde{T}_e| = 0, \tag{14}$$

Let's choose the position and force scaling factors $\alpha = 1$, $\beta = \frac{\varrho_m}{\varrho_s}$, and reconsider the control law in (10) with the human/environment force modeled as (8), one can have

$$\begin{aligned}
 \bar{T}_m &= K_p \widehat{e}_{mp} + K_{fm} \widehat{e}_{mf} = K_p \left(e_{mp} + \frac{K_f}{K_p} e_{mf} \right) \\
 &= K_p \left(\frac{K_f}{K_p} \varrho_m (\widehat{q}_s(t - T_2(t)) - \widehat{q}_m(t)) + \left(1 + \frac{K_f}{K_p} \varrho_m \rho \right) (\widehat{q}_s(t - T_2(t)) - \widehat{q}_m(t)) \right), \tag{15}
 \end{aligned}$$

Let's define $A_1 = \frac{K_f}{K_p} \varrho_m$, $B_1 = I + \frac{K_f}{K_p} \varrho_m \rho$, then (15) turns into

$$\bar{T}_m = K_p (A_1 (\widehat{q}_s(t - T_2(t)) - \widehat{q}_m(t)) + B_1 (\widehat{q}_s(t - T_2(t)) - \widehat{q}_m(t))), \tag{16}$$

Similarly, one can get

$$\bar{T}_s = K_p \widehat{e}_{sp} - K_f \widehat{e}_{sf} = K_p \left(\frac{K_f}{K_p} \varrho_s (\widehat{q}_m(t - T_1(t)) - \widehat{q}_s(t)) + \left(1 + \frac{K_f}{K_p} \varrho_s \rho \right) (\widehat{q}_m(t - T_1(t)) - \widehat{q}_s(t)) \right), \tag{17}$$

Let's define $A_2 = \frac{K_f}{K_p} \varrho_s$, $B_2 = I + \frac{K_f}{K_p} \varrho_s \rho$, then (17) turns into

$$\bar{T}_s = K_p (A_2 (\widehat{q}_m(t - T_1(t)) - \widehat{q}_s(t)) + B_2 (\widehat{q}_m(t - T_1(t)) - \widehat{q}_s(t))), \tag{18}$$

Now, let's define a Lyapunov function $V(t)$ as

$$V(t) = V_1(t) + V_2(t) + V_3(t) + V_4(t), \tag{19}$$

where

$$\begin{aligned}
 V_1(t) &= \frac{1}{2} \widehat{q}_m^T(t) \widehat{M}_m(\widehat{q}_m(t)) \widehat{q}_m(t) + \frac{1}{2} \frac{B_1}{B_2} \widehat{q}_s^T(t) \widehat{M}_s(\widehat{q}_s(t)) \widehat{q}_s(t), \\
 V_2(t) &= - \int_0^t \widehat{q}_m^T(\eta) \widehat{T}_h(\eta) d\eta + \rho_h - \int_0^t \widehat{q}_s^T(\eta) \widehat{T}_e(\eta) d\eta + \rho_e, \\
 V_3(t) &= \frac{1}{2} K_p B_1 (\widehat{q}_m(t) - \widehat{q}_s(t))^T (\widehat{q}_m(t) - \widehat{q}_s(t)), \\
 V_4(t) &= \frac{1}{1 - \dot{T}_1(t)} \frac{1}{2} \frac{B_1}{B_2} K_p A_2 \int_{t-T_1(t)}^t |\widehat{q}_m(\eta)|^2 d\eta + \frac{1}{1 - \dot{T}_2(t)} \frac{1}{2} K_p A_1 \int_{t-T_2(t)}^t |\widehat{q}_s(\eta)|^2 d\eta.
 \end{aligned}$$

Using Property 2 in Section 2, the time derivative of $V_1(t) + V_2(t)$ can be written as

$$\begin{aligned}
 \dot{V}_1(t) + \dot{V}_2(t) &= \widehat{q}_m^T(t) (\bar{T}_m - K_{bm} \widehat{q}_m(t)) + \frac{B_1}{B_2} \widehat{q}_s^T(t) (\bar{T}_s - K_{bs} \widehat{q}_s(t)) = K_p A_1 \widehat{q}_m^T(t) \widehat{q}_s(t - T_2(t)) \\
 &\quad + K_p B_1 \widehat{q}_m^T(t) (\widehat{q}_s(t - T_2(t)) - \widehat{q}_m(t)) - (K_{bm} + K_p A_1) |\widehat{q}_m(t)|^2 \\
 &\quad + \frac{B_1}{B_2} K_p A_2 \widehat{q}_s^T(t) \widehat{q}_m(t - T_1(t)) + K_p B_1 \widehat{q}_s^T(t) (\widehat{q}_m(t - T_1(t)) - \widehat{q}_s(t)) \\
 &\quad - \left(K_{bs} + \frac{B_1}{B_2} K_p A_2 \right) |\widehat{q}_s(t)|^2, \tag{20}
 \end{aligned}$$

Also, the time derivate of $V_3(t)$ is given by

$$\dot{V}_3(t) = K_p B_1 (\widehat{q}_m(t) - \widehat{q}_s(t))^T (\widehat{q}_m(t) - \widehat{q}_s(t)), \tag{21}$$

By adding (20) and (21), one can get

$$\begin{aligned}
 \dot{V}_1(t) + \dot{V}_2(t) + \dot{V}_3(t) &= -(K_{bm} + K_p A_1) |\widehat{q}_m(t)|^2 - \left(K_{bs} + \frac{B_1}{B_2} K_p A_2 \right) |\widehat{q}_s(t)|^2 \\
 &\quad + K_p A_1 \widehat{q}_m^T(t) \widehat{q}_s(t - T_2(t)) + \frac{B_1}{B_2} K_p A_2 \widehat{q}_s^T(t) \widehat{q}_m(t - T_1(t)) \\
 &\quad + K_p B_1 \widehat{q}_m^T(t) (\widehat{q}_s(t - T_2(t)) - \widehat{q}_s(t)) + K_p B_1 \widehat{q}_s^T(t) (\widehat{q}_m(t - T_1(t)) - \widehat{q}_m(t)), \tag{22}
 \end{aligned}$$

Since $\widehat{q}_m(t - T_1(t)) - \widehat{q}_m(t) = - \int_{-T_1(t)}^0 \widehat{q}_m(t + \eta) d\eta$, $\widehat{q}_s(t - T_2(t)) - \widehat{q}_s(t) = - \int_{-T_2(t)}^0 \widehat{q}_s(t + \eta) d\eta$, and the bounds

$$K_p A_1 \widehat{q}_m^T(t) \widehat{q}_s(t - T_2(t)) \leq \frac{1}{2} K_p A_1 \left(|\widehat{q}_m(t)|^2 + |\widehat{q}_s(t - T_2(t))|^2 \right), \tag{23a}$$

$$\frac{B_1}{B_2} K_p A_2 \widehat{q}_s^T(t) \widehat{q}_m(t - T_1(t)) \leq \frac{1}{2} \frac{B_1}{B_2} K_p A_2 \left(|\widehat{q}_s(t)|^2 + |\widehat{q}_m(t - T_1(t))|^2 \right), \tag{23b}$$

Then, one can further write (22) as

$$\begin{aligned}
 \dot{V}_1(t) + \dot{V}_2(t) + \dot{V}_3(t) &\leq - \left(K_{bm} + \frac{1}{2} K_p A_1 \right) |\widehat{q}_m(t)|^2 - \left(K_{bs} + \frac{1}{2} \frac{B_1}{B_2} K_p A_2 \right) |\widehat{q}_s(t)|^2 \\
 &\quad - K_p B_1 \widehat{q}_s^T(t) \int_{-T_1(t)}^0 \widehat{q}_m(t + \eta) d\eta - K_p B_1 \widehat{q}_m^T(t) \int_{-T_2(t)}^0 \widehat{q}_s(t + \eta) d\eta \\
 &\quad + \frac{1}{2} \frac{B_1}{B_2} K_p A_2 |\widehat{q}_m(t - T_1(t))|^2 + \frac{1}{2} K_p A_1 |\widehat{q}_s(t - T_2(t))|^2, \tag{24}
 \end{aligned}$$

In addition, the time derivate of $V_4(t)$ is calculated as

$$\begin{aligned} \dot{V}_4(t) &= \frac{1}{1 - \dot{T}_1(t)} \frac{1}{2} \frac{B_1}{B_2} K_p A_2 \left(|\hat{q}_m(t)|^2 - (1 - \dot{T}_1(t)) |\hat{q}_m(t - T_1(t))|^2 \right) \\ &\quad + \frac{1}{1 - \dot{T}_2(t)} \frac{1}{2} K_p A_1 \left(|\hat{q}_s(t)|^2 - (1 - \dot{T}_2(t)) |\hat{q}_s(t - T_2(t))|^2 \right) \\ &= \frac{1}{1 - \dot{T}_1(t)} \frac{1}{2} \frac{B_1}{B_2} K_p A_2 |\hat{q}_m(t)|^2 + \frac{1}{1 - \dot{T}_2(t)} \frac{1}{2} K_p A_1 |\hat{q}_s(t)|^2 - \frac{1}{2} \frac{B_1}{B_2} K_p A_2 |\hat{q}_m(t - T_1(t))|^2 \\ &\quad - \frac{1}{2} K_p A_1 |\hat{q}_s(t - T_2(t))|^2, \end{aligned} \tag{25}$$

Combining (24) with (25), one can get

$$\begin{aligned} \dot{V}(t) &= \dot{V}_1(t) + \dot{V}_2(t) + \dot{V}_3(t) + \dot{V}_4(t) \leq - \left(K_{bm} + \frac{1}{2} K_p A_1 - \frac{1}{1 - \dot{T}_1(t)} \frac{1}{2} \frac{B_1}{B_2} K_p A_2 \right) |\hat{q}_m(t)|^2 \\ &\quad - \left(K_{bs} + \frac{1}{2} \frac{B_1}{B_2} K_p A_2 - \frac{1}{1 - \dot{T}_2(t)} \frac{1}{2} K_p A_1 \right) |\hat{q}_s(t)|^2 - K_p B_1 \hat{q}_s^T(t) \int_{-T_1(t)}^0 \hat{q}_m(t + \eta) d\eta \\ &\quad - K_p B_1 \hat{q}_m^T(t) \int_{-T_2(t)}^0 \hat{q}_s(t + \eta) d\eta, \end{aligned} \tag{26}$$

Applying Lemma 1 in [14], one has

$$\begin{aligned} &\int_0^t \left(-K_p B_1 \hat{q}_s^T(t) \int_{-T_1(t)}^0 \hat{q}_m(t + \eta) d\eta - K_p B_1 \hat{q}_m^T(t) \int_{-T_2(t)}^0 \hat{q}_s(t + \eta) d\eta \right) dt \\ &\leq \frac{K_p B_1}{2} \left(\omega_1 + \frac{T_{1\max}^2}{\omega_2} \right) |\hat{q}_m(t)|^2 + \frac{K_p B_1}{2} \left(\omega_2 + \frac{T_{2\max}^2}{\omega_1} \right) |\hat{q}_s(t)|^2. \end{aligned}$$

Then, Integrating $\dot{V}(t)$ in (26) from zero to t , yields

$$V(t) - V(0) \leq -\mu_1 |\hat{q}_m(t)|^2 - \mu_2 |\hat{q}_s(t)|^2, \tag{27}$$

where

$$\begin{aligned} \mu_1 &= K_{bm} + \frac{1}{2} K_p A_1 - \frac{1}{1 - \dot{T}_1(t)} \frac{1}{2} \frac{B_1}{B_2} K_p A_2 - \frac{K_p B_1}{2} \left(\omega_1 + \frac{T_{1\max}^2}{\omega_2} \right), \\ \mu_2 &= K_{bs} + \frac{1}{2} \frac{B_1}{B_2} K_p A_2 - \frac{1}{1 - \dot{T}_2(t)} \frac{1}{2} K_p A_1 - \frac{K_p B_1}{2} \left(\omega_2 + \frac{T_{2\max}^2}{\omega_1} \right). \end{aligned}$$

If we choose the controller parameters K_p, K_f, K_{bm}, K_{bs} to satisfy $\mu_1 > 0, \mu_2 > 0$, then $\hat{q}_m(t), \hat{q}_s(t), \hat{q}_m(t) - \hat{q}_s(t) \in L_2 \cap L_\infty$. Combined with (14), we have $\dot{q}_m(t), \dot{q}_s(t), q_m(t) - q_s(t) \in L_2 \cap L_\infty$.

Let's reconsider e_{mp} as

$$\begin{aligned} e_{mp} &= q_s(t - T_2(t)) - q_m(t) = q_s(t - T_2(t)) - q_s(t) + q_s(t) - q_m(t) \\ &= - \int_0^{T_2(t)} \hat{q}_s(t - \eta) d\eta + q_s(t) - q_m(t). \end{aligned} \tag{28}$$

Since $q_s(t) - q_m(t) \in L_2 \cap L_\infty$, Using Schwartz's inequality, $\int_0^{T_2(t)} \hat{q}_s(t - \eta) d\eta \leq T_{2\max}^{\frac{1}{2}} \|\dot{q}_s(t)\|_2 \in L_2 \cap L_\infty$, where $\|\dot{q}_s(t)\|_2$ stands for the Euclidian 2-norm of the vector $\dot{q}_s(t) \in R^n$. Thus, $e_{mp} \in L_2 \cap L_\infty$, similarly, we can show $e_{sp} = q_m(t - T_1(t)) - q_s(t) \in L_2 \cap L_\infty$. This completes the proof.

One can notice that the conditions 5 and 6 of the Theorem 1 are the persistency criteria for the deployed IEAOB, the derivation of the conditions 5 and 6 is an extension of the results in [46, 47]. These

two conditions look complicated and hard to check before implementation, however, it can be viewed in another easy way based on the results in [46, 47]: If the desired trajectory is persistently exciting, the IEAOB would be uniformly stable provided that the inertia matrix $M_*(q_*)$ is positive definite.

4. Simulation study

In this section, computer simulation will be carried out to illustrate the effectiveness of the proposed control scheme. Both the master and slave robots are considered to be planar two-link manipulators. The dynamic model of a 2 DOF nonlinear teleoperation system in the joint space is defined as

$$M_m(q_m, \theta_m) \ddot{q}_m + V_m(q_m, \dot{q}_m, \theta_m) \dot{q}_m + g_m(q_m, \theta_m) + T_{f_m} = T_m + T_h, \tag{29a}$$

$$M_s(q_s, \theta_s) \ddot{q}_s + V_s(q_s, \dot{q}_s, \theta_s) \dot{q}_s + g_s(q_s, \theta_s) + T_{f_s} = T_s + T_e, \tag{29b}$$

where T_{f_*} is defined in (2),

$$\theta_* = \begin{bmatrix} \theta_{*1} \\ \theta_{*2} \end{bmatrix} = \begin{bmatrix} m_{*1} l_{*1}^2 \\ m_{*2} l_{*2}^2 \end{bmatrix},$$

$$M_*(q_*, \theta_*) = \begin{bmatrix} \theta_{*1} + 2\theta_{*2} + 2\theta_{*2}\cos(q_{*2}) & \theta_{*2} + \theta_{*2}\cos(q_{*2}) \\ \theta_{*2} + \theta_{*2}\cos(q_{*2}) & \theta_{*2} \end{bmatrix},$$

$$V_*(q_*, \dot{q}_*, \theta_*) = \begin{bmatrix} -2\theta_{*2}\dot{q}_{*2}\sin(q_{*2}) & -\theta_{*2}\dot{q}_{*2}\sin(q_{*2}) \\ \theta_{*2}\dot{q}_{*1}\sin(q_{*2}) & 0 \end{bmatrix},$$

where $* = m/s, l_{*1} = l_{*2}$ are the lengths of the first and the second links, m_{*1} and m_{*2} are the masses of the first and the second links, and we assume the robots operate in a horizontal plane, and as such $g_*(q_*, \theta_*)$ is zero.

4.1. Initial conditions

The sample time is set to 1.0 ms. The actual values of the robot dynamical parameter and friction coefficients are $\theta_{*1} = 0.1\text{kgm}^2, \theta_{*2} = 0.2\text{kgm}^2, v_{v_*} = 2.5e - 3, v_{c_*} = 5.0e - 3$. The time-varying delays are simulated in PC. The forward and feedback time delays are chosen as random variables in the range of [0.1, 0.3] s with $\dot{T}_{1,2}(t) \leq 0.5$. In the simulation, human operator manipulates the master manipulator and the slave manipulator makes contact with the environment at around 0.3 rad.

In order to demonstrate the superiority of the proposed approach, we assume that there is no parameter variation ($\theta_{m1}, \theta_{m2}, v_{v_m}, v_{c_m}$ are set to the actual values) for the master robot, while 20% parameter variation ($\theta_{s1}, \theta_{s2}, v_{v_s}, v_{c_s}$ are 20% larger than the actual values) is considered in the slave robot. The parameters for the adaptive observer-based robust scaled 4-CH control with damping injection proposed in this paper in the presence of time delay, and model uncertainties and disturbances are as follows:

The human insert torque to the master manipulator is shown in Fig. 2. The parameters of the position and force controllers for the master and slave robots are selected as $K_p = \begin{bmatrix} 0.3 & 0 \\ 0 & 0.3 \end{bmatrix}$

and $K_f = \begin{bmatrix} 0.3 & 0 \\ 0 & 0.3 \end{bmatrix}$. The damping coefficients for the master and slave robots are selected as

$K_{bm} = \begin{bmatrix} 3 & 0 \\ 0 & 3 \end{bmatrix}, K_{bs} = \begin{bmatrix} 3 & 0 \\ 0 & 3 \end{bmatrix}$. The human and environment model parameters are selected as

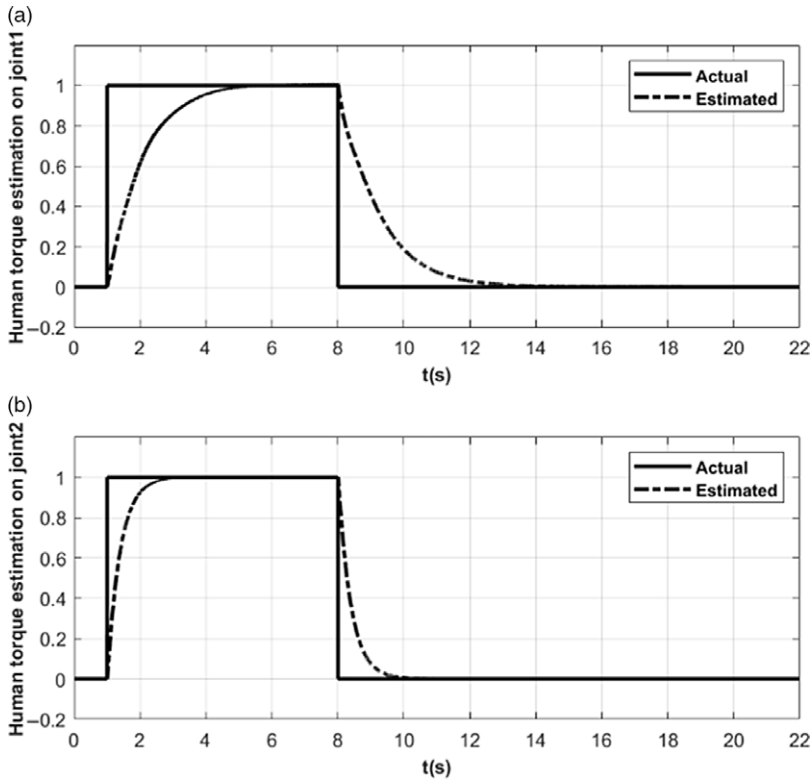


Figure 2. The human insert torque to the master manipulator and its estimation by IEAOB.

$\mathcal{O}_m = \mathcal{O}_s = \begin{bmatrix} 0.5 & 0 \\ 0 & 0.5 \end{bmatrix}, \rho = 1$. From the filtering theory, the initial filtered state estimates are the expected values of these states at the beginning of control. Hence, for the robotic manipulator starting at rest and at origin, the initial filtered states: $q_{m_0} = 0, q_{s_0} = 0, \dot{q}_{m_0} = 0, \dot{q}_{s_0} = 0$. Hence, the initial conditions of IEAOB for the master and slave robots, when measurement noises ($N \sim (0, 1.0e - 4)$) are considered at both sides of the teleoperation system and 20% dynamical parameter variation is considered for the slave robot, are chosen respectively as

$$\hat{X}_{m_0} = (0, 0, 0, 0, 0.1, 0.2, 2.5e - 3, 5.0e - 3, 2.5e - 3, 5.0e - 3, 0, 0)'$$

$$R_m = \text{diag} \{1.0e - 4, 1.0e - 4\},$$

$$Q_m = \text{diag}\{1.0e - 7, 1.0e - 7, 1.0e - 7, 1.0e - 7, 1.0e - 2, 1.0e - 2, 1.0e - 2, 1.0e - 2, 1.0e - 2, 1.0e - 2, 1.0e - 2, 8.0e - 7, 1.0e - 6\},$$

$$P_{m_0} = \text{diag}\{1.0e - 7, 1.0e - 7, 1.0e - 7, 1.0e - 7, 1.0e - 4, 1.0e - 4, 1.0e - 4, 1.0e - 4, 1.0e - 4, 1.0e - 4, 1.0e - 4, 1.0e - 7, 1.0e - 7\}.$$

$$\hat{X}_{s_0} = (0, 0, 0, 0, 0.12, 0.24, 3.0e - 3, 6.0e - 3, 3e - 3, 6e - 3, 0, 0)'$$

$$R_s = \text{diag} \{1.0e - 4, 1.0e - 4\},$$

$$Q_s = \text{diag}\{1.0e - 7, 1.0e - 7, 1.0e - 7, 1.0e - 7, 1.0e - 2, 1.0e - 2, 1.0e - 2, 1.0e - 2, 1.0e - 2, 1.0e - 2, 1.0e - 2, 8.0e - 7, 1.0e - 6\},$$

$$P_{s_0} = \text{diag}\{1.0e - 7, 1.0e - 7, 1.0e - 7, 1.0e - 7, 1.0e - 4, 1.0e - 4, 1.0e - 4, 1.0e - 4, 1.0e - 4, 1.0e - 4, 1.0e - 4, 1.0e - 7, 1.0e - 7\}.$$

Based on the selected parameters for the simulation, it is easy to show, as below, that they satisfy the conditions 1, 2, 3, 4 of the Theorem 1.

$$\mu_1 = K_{bm} + \frac{1}{2}K_pA_1 - \frac{1}{1 - \dot{T}_1(t)} \frac{1}{2} \frac{B_1}{B_2} K_pA_2 - \frac{K_pB_1}{2} \left(\omega_1 + \frac{T_{1\max}^2}{\omega_2} \right) \geq \begin{bmatrix} 2.772 & 0 \\ 0 & 2.772 \end{bmatrix} > 0,$$

$$\mu_2 = K_{bs} + \frac{1}{2} \frac{B_1}{B_2} K_pA_2 - \frac{1}{1 - \dot{T}_2(t)} \frac{1}{2} K_pA_1 - \frac{K_pB_1}{2} \left(\omega_2 + \frac{T_{2\max}^2}{\omega_1} \right) \geq \begin{bmatrix} 2.772 & 0 \\ 0 & 2.772 \end{bmatrix} > 0, \text{ where}$$

$$\dot{T}_{1,2}(t) \leq 0.5, T_{1\max} = T_{2\max} = 0.3, \omega_1 = \omega_2 = 0.5,$$

$$\alpha_1 I \leq Q_m(t) \leq \alpha_2 I, \beta_1 I \leq Q_s(t) \leq \beta_2 I, \text{ where } \alpha_1 = \beta_1 = 1.0e - 7 > 0, \alpha_2 = \beta_2 = 1.0e - 2 > 0,$$

$$\alpha_3 I \leq R_m(t) \leq \alpha_4 I, \beta_3 I \leq R_s(t) \leq \beta_4 I, \text{ where } \alpha_3 = \beta_3 = 1.0e - 4 > 0, \alpha_4 = \beta_4 = 1.0e - 4 > 0.$$

4.2. Simulation results and analysis

In this simulation, the performance of the proposed teleoperation approach under the circumstance of measurement noise: $N \sim (0, 1.0e-4)$ at both ends of the teleoperation system and parameter variation: 20% larger than the actual parameters at the slave side of the teleoperation system is examined. Figures 2 and 7 depict the human and environment rendered torques to the master and slave manipulators and the torque estimations by IEAOB, it is easy to observe that the rendered torques are estimated with an acceptable accuracy by IEAOB under no requirement of any human/environment dynamical model information. Figures 5 and 10 illustrate the master and slave robot dynamical parameters and friction coefficients estimation performances by IEAOB, respectively. As there is no parameter variation assumed at the master end, the parameter convergence curves almost maintain unchanged in Fig. 5 during the simulation, while the parameter estimation curves for the slave robot in Fig. 10 asymptotically converge to the actual values ($\theta_{s1} = 0.1, \theta_{s2} = 0.2, v_{v_{s-1}} = v_{v_{s-2}} = 2.5e - 3, v_{c_{s-1}} = v_{c_{s-2}} = 5.0e - 3$) due to 20% parameter variation. Figures 3-4 and 8-9 describe the position and velocity estimation errors by IEAOB at the master and slave ends, respectively. As expected, the error trajectories converge to zero eventually. It is observed from Fig. 3 that the peak point for the second joint is higher than that of the first joint, which results from the sudden contact with the environment. However, when the scale of the estimation error is taken into account, the error is relatively small compared to the actual position. Furthermore, Fig. 6 and Fig. 11 show the force and position synchronization errors at the master and slave sides respectively, there are position error peak points in these two figures, which result from the sudden contact with the environment, but the two figures demonstrate that even in the large time-varying delays, the teleoperation system still has accurate trajectory tracking performances with very little steady-state errors by using the proposed control algorithm. As for the method to reduce the error for the force estimation for the presented IEAOB, one way is to deploy the high-order IEAOB for estimation, the result for this was shown in [48], it will significantly increase the accuracy. However, at the meantime, it will increase the calculation difficulty. Hence, one needs to take a balanced view to consider this when applying it to real-world applications.

In summary, the simulation results illustrate that the proposed scaled 4-CH control scheme with the damping injection can achieve accurate trajectory tracking at the master and slave sides, respectively, as well as simultaneous human force estimation and parameter adaptation for nonlinear master and slave systems in the presence of time-varying delays, robot parameter variations and measurement noises.

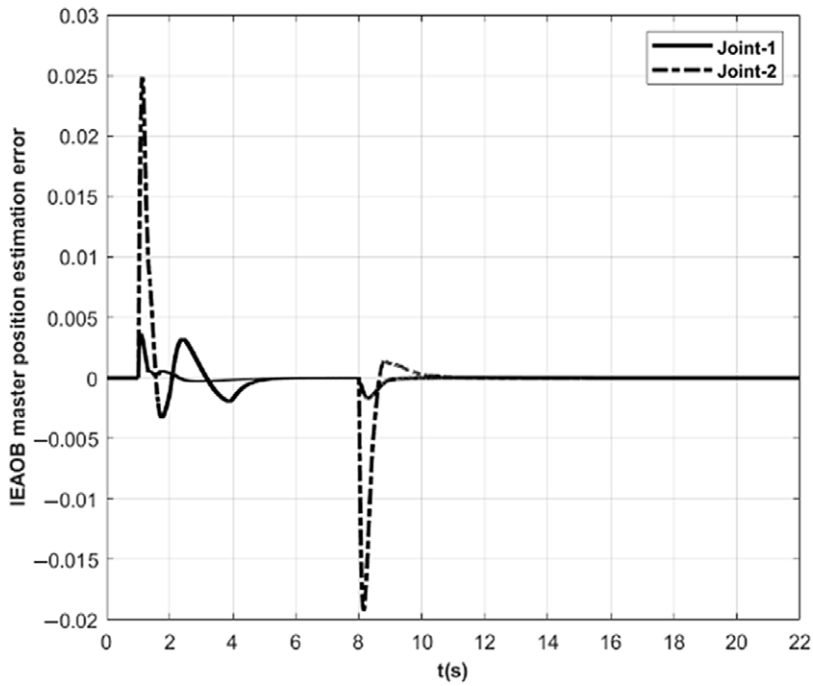


Figure 3. The master position estimation error by IEAOB.

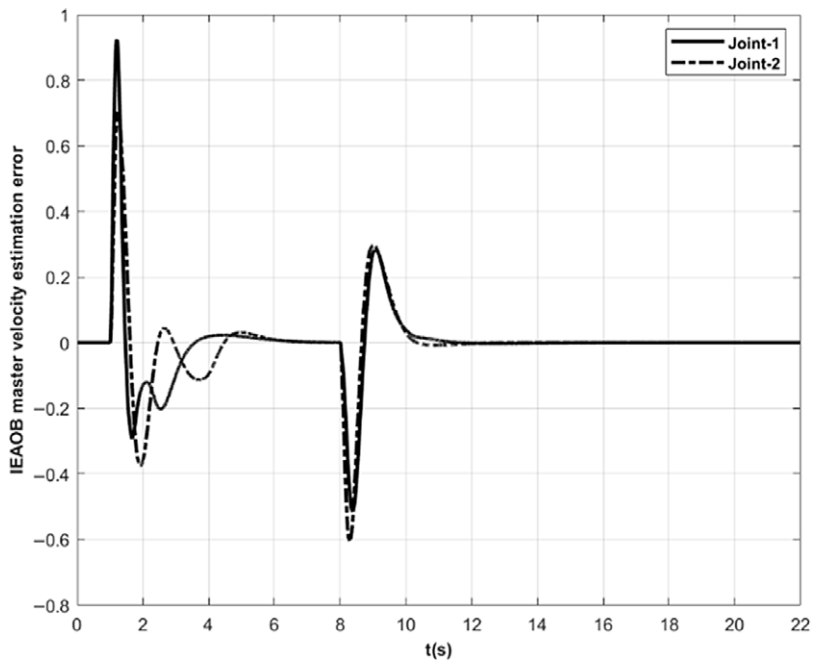


Figure 4. The master velocity estimation error by IEAOB.

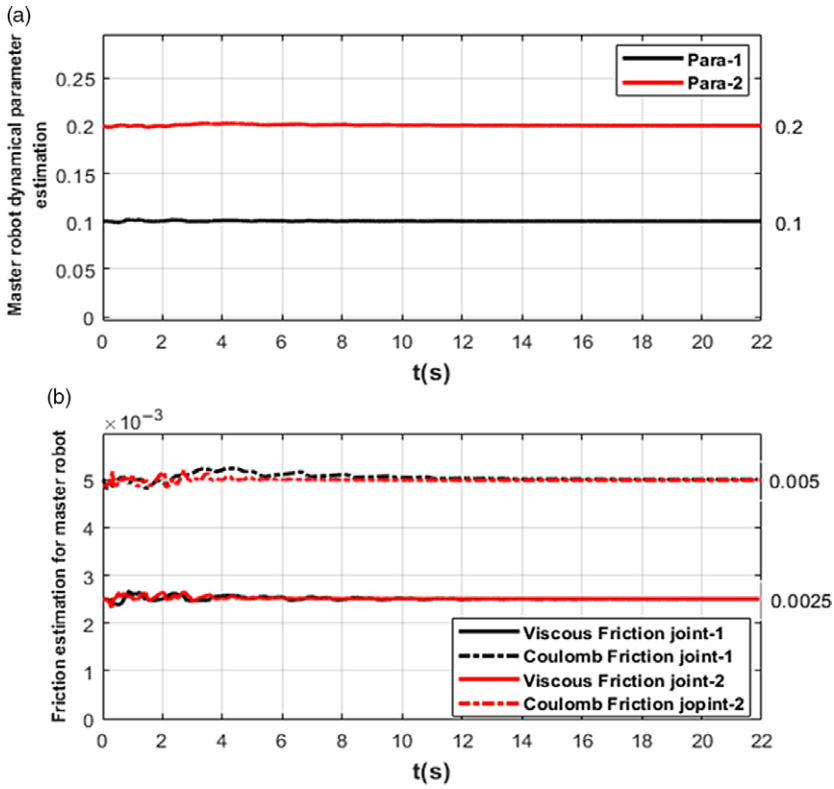


Figure 5. The master robot parameter estimation performance by IEAOB.

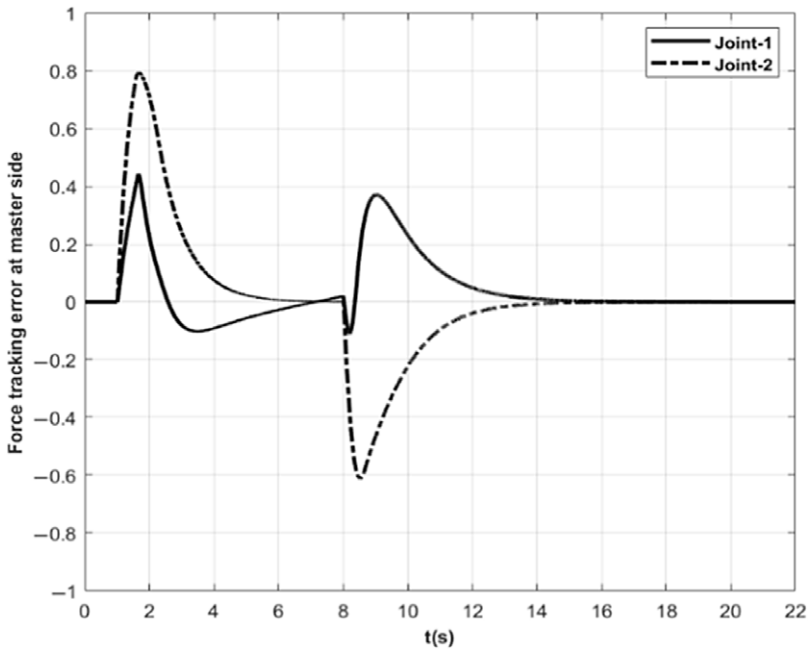


Figure 6. Force synchronization error at the master side.

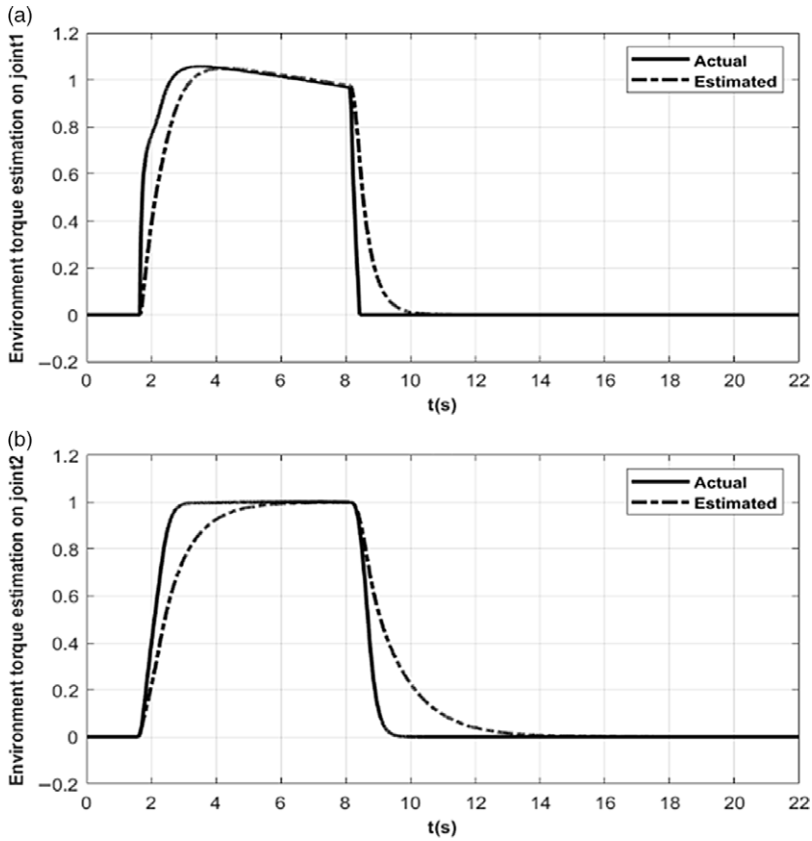


Figure 7. The environment torque to the slave manipulator and its estimation by IEAOB.

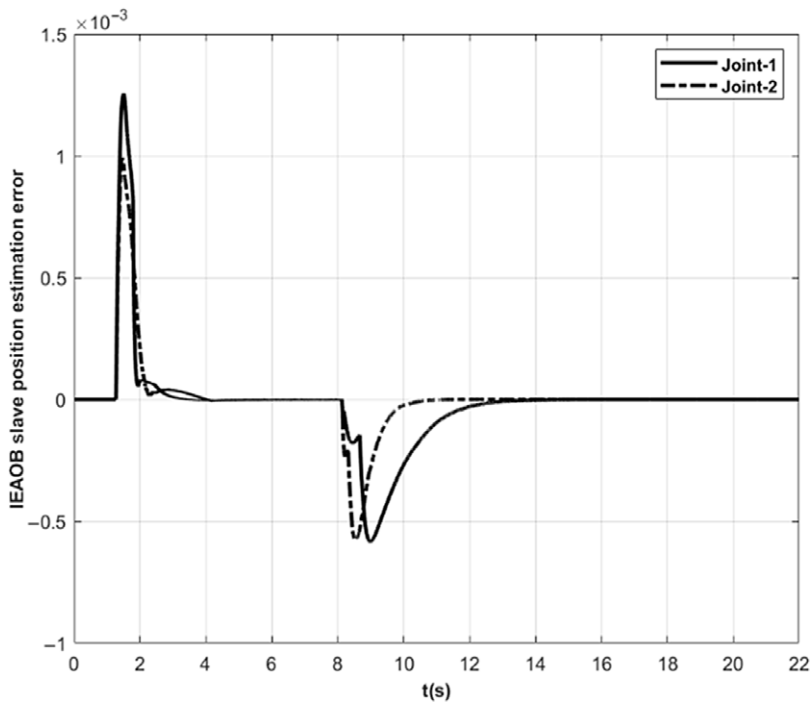


Figure 8. The slave position estimation error by IEAOB.

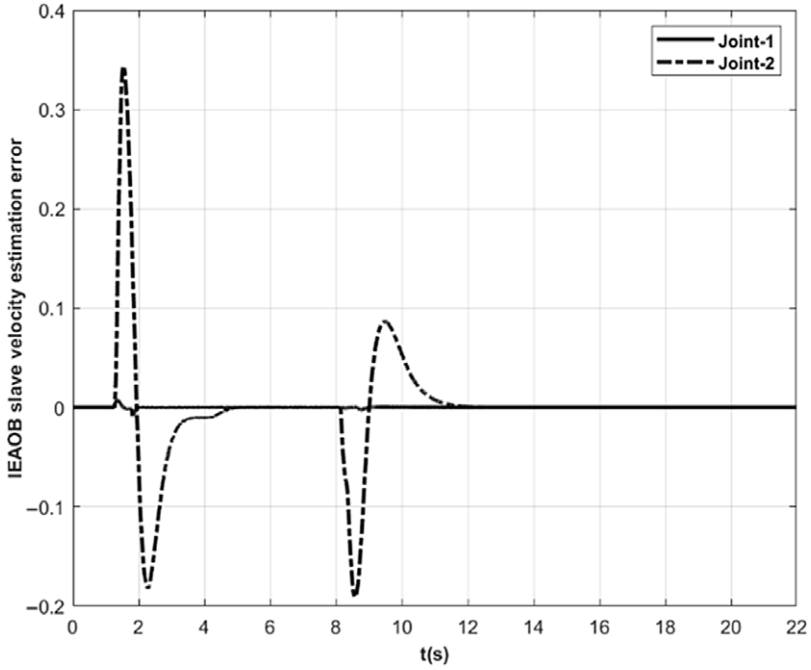


Figure 9. The slave velocity estimation error by IEAOB.

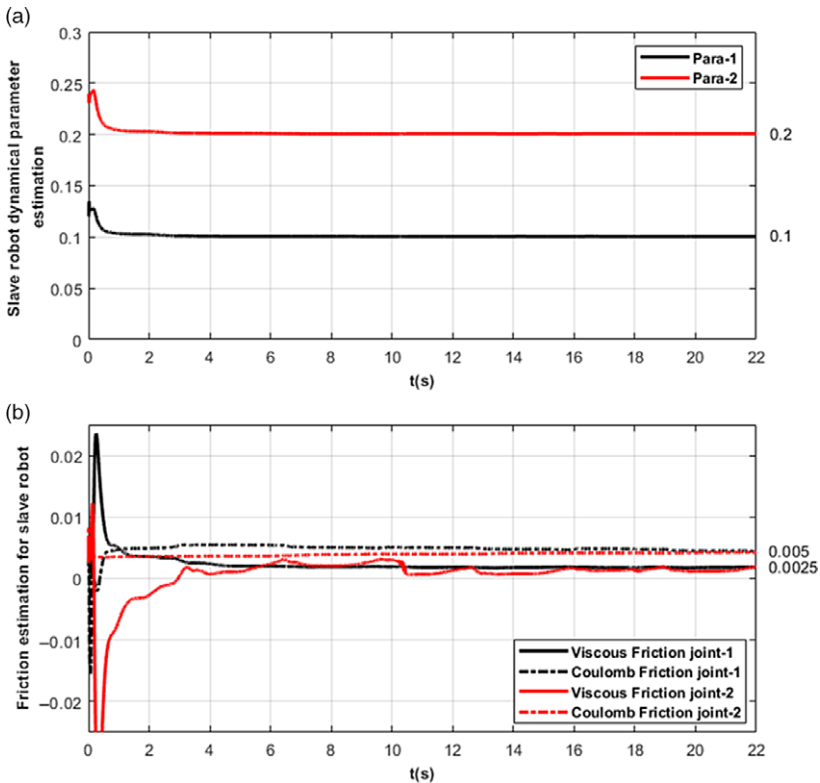


Figure 10. The slave robot parameter estimation performance by IEAOB.

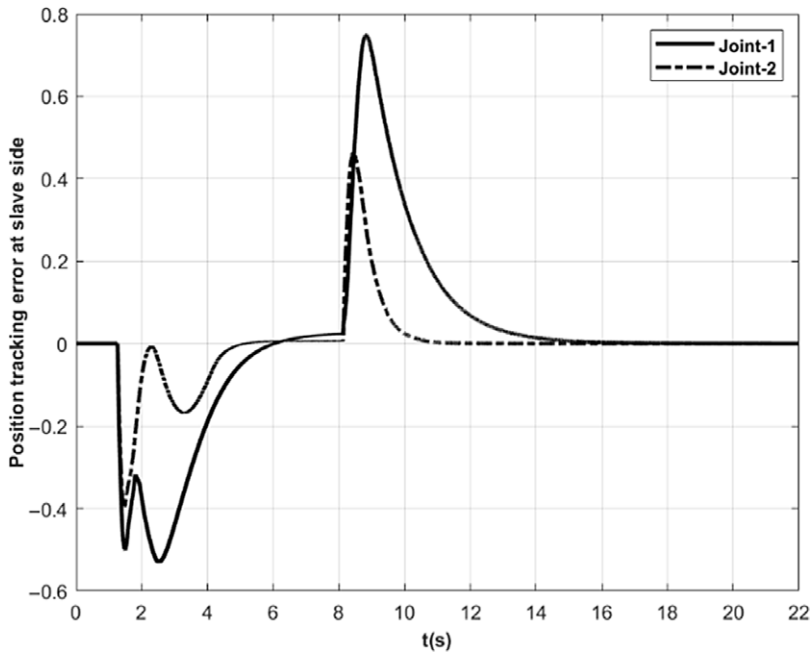


Figure 11. Position synchronization error at the slave side.

5. Conclusion

In this article, the major control issues in a nonlinear bilateral teleoperation system are considered and addressed, including dynamic uncertainties, external force acquirement, and time-varying communication delays. A novel scaled 4-CH control scheme with the damping injection is developed to handle the time-varying delay and improve the position and force tracking performances in addition to guaranteeing the passivity of the communication channels and accordingly the stability of the whole system. Meanwhile, the IEAOB is utilized to eliminate the perturbations caused by the internal parameter uncertainties and external disturbance (measurement noise) while obtaining accurate environment/operator force estimation. By applying the proper Lyapunov function, the whole master-slave system stability is analyzed and the stability conditions are deduced. The simulation result on a 2-DOF nonlinear teleoperation system demonstrates the feasibility of the proposed control algorithm under time-varying time delays. In the future, the experiments will be carried out to validate the proposed method in practical use. Meanwhile, actuator saturation issue will be studied for the proposed method and extending these results from bilateral teleoperation to multilateral teleoperation will also be a future research direction.

References

- [1] R. Taylor and D. Stojanovici, "Medical robotics in computer-integrated surgery," *IEEE Trans. Robot. Autom.* **19**, 765–781 (2003).
- [2] C. Passenbarg, A. Peer and M. Buss, "A survey of environment-, operator-, and task-adapted controllers for teleoperation systems", *Mechatronics* **20**, 787–801 (2010).
- [3] D. A. Lawrence, "Towards force reflecting teleoperation over the Internet," in *Proc. IEEE Int. Conf. Robot. Autom.*, (Nice, France, 1992), pp. 1406–1411.
- [4] A. Ghavifekr, A. Ghiasi, and M. Badamchizadeh. "Discrete-time control of bilateral teleoperation systems: a review." *Robotica* **36**(4), 552–569 (2018).
- [5] A. Ghavifekr, et al. "Exponential stability of bilateral sampled-data teleoperation systems using multirate approach." *ISA Trans.* **105**, 190–197 (2020).
- [6] G. Niemeyer and J.-J. E. Slotine, "Stable adaptive teleoperation," *IEEE J. Ocean. Eng.* **16**(1), 152–162 (1991).

- [7] N. Chopra, M. W. Spong, S. Hirche, and M. Buss, "Bilateral teleoperation over the Internet: The time varying delay problem," in *Proc. Amer. Control Conf.*, pp. 155–160 (2003).
- [8] R. Lozano, N. Chopra, and M. W. Spong, "Passivation of force reflecting bilateral teleoperators with time varying delay," in *Proc. Mechatronics Forum*, pp. 954–962, (2002).
- [9] Y. Ye and P. X. Liu, "Improving trajectory tracking in wave-variable-based teleoperation," *IEEE/ASME Trans. Mechatron.* **15**(2), 321–326 (2010).
- [10] H. Li and K. Kawashima, "Achieving stable tracking in wave-variable based teleoperation," *IEEE/ASME Trans. Mechatron.* **19**(5), 1574–1582 (2014).
- [11] D. Sun, F. Naghdy, and H. Du, "Wave-variable-based passivity control of four-channel nonlinear bilateral teleoperation system under time delays," *IEEE/ASME Trans. Mechatron.* **21**(1), 238–253 (2016).
- [12] Z. Chen, F. Huang, W. Sun, and W. Song, "An improved wave variable based four-channel control design in bilateral teleoperation system for time-delay compensation," *IEEE Access* **6**, 12848–12857 (2018).
- [13] E. Nuño, R. Ortega, N. Barabanov, and L. Basañez, "A globally stable PD controller for bilateral teleoperators," *IEEE Trans. Robot.* **24**(3), 753–758 (2008).
- [14] E. Nuño, L. Basañez, R. Ortega, and M. W. Spong, "Position tracking for non-linear teleoperators with variable time delay," *Int. J. Robot. Res.* **28**(7), 895–910 (2009).
- [15] Y. Yang, D. Constantinescu, and Y. Shi, "Input-to-state stable bilateral teleoperation by dynamic interconnection and damping injection: theory and experiments," *IEEE Trans. Ind. Electron.* **67**(1), 790–799 (2020).
- [16] L. Chan, F. Naghdy, and D. Stirling, "Application of adaptive controllers in teleoperation systems: A survey," *IEEE Trans. Human-Mach. Systems.* **44**(3), 337–352 (2014).
- [17] E. Nuño, L. Basañez, and R. Ortega, "Passivity-based control for bilateral teleoperation: A tutorial," *Automatica* **47**(3), 485–495 (2011).
- [18] L. Chan, F. Naghdy, and D. Stirling, "Extended active observer for force estimation and disturbance rejection of robotic manipulators," *Rob. Auton. Sys.* **61**, 1277–1287 (2013).
- [19] L. Chan, F. Naghdy, and D. Stirling, "Position and force tracking for non-linear haptic telemanipulator under varying delays with an improved extended active observer," *Robot. Auton. Sys.* **75**, 145–160 (2016).
- [20] R. Cortesão, J. Park, and O. Khatib, "Real-time adaptive control for haptic telemanipulation with kalman active observers," *IEEE Trans. Robot.* **22**(5), 987–999 (2006).
- [21] Z. Chen, B. Yao, and Q. Wang, "Accurate motion control of linear motors with adaptive robust compensation of nonlinear electromagnetic field effect," *IEEE/ASME Trans. Mechatron.* **18**(3), 1122–1129 (2013).
- [22] W. Sun, H. Pan, and H. Gao, "Filter-based adaptive vibration control for active vehicle suspensions with electro-hydraulic actuators," *IEEE Trans. Veh. Technol.* **65**(6), 4619–4626 (2016).
- [23] J. Yao and W. Deng, "Active disturbance rejection adaptive control of hydraulic servo systems," *IEEE Trans. Ind. Electron.* **64**(10), 8023–8032 (2017).
- [24] J. Yao, W. Deng, and Z. Jiao, "RISE-based adaptive control of hydraulic systems with asymptotic tracking," *IEEE Trans. Autom. Sci. Eng.* **14**(3), 1524–1531 (2017).
- [25] H. C. Cho and J. H. Park, "Stable bilateral teleoperation under a time delay using a robust impedance control," *Mechatronics* **15**(5), 611–625 (2005).
- [26] Z. Chen, B. Yao, and Q. Wang, " μ -synthesis based adaptive robust control of linear motor driven stages with high-frequency dynamics: A case study," *IEEE/ASME Trans. Mechatron.* **20**(3), 1482–1490 (2015).
- [27] C. A. L. Martínez, R. van de Molengraft, S. Weiland, and M. Steinbuch, "Switching robust control for bilateral teleoperation," *IEEE Trans. Control Syst. Technol.* **24**(1), 172–188 (2016).
- [28] B. Jing, J. Na, G. Gao, and C. Yang, "Robust adaptive control for bilateral teleoperation systems with guaranteed parameter estimation," in *Proc. Int. Conf. Adv. Robot. Mechatronics*, pp. 32–37, (2016).
- [29] C. Cheng, W. Xu, and J. Shang, "Distributed-torque-based independent joint tracking control of a redundantly actuated parallel robot with two higher kinematic pairs," *IEEE Trans. Industr. Electron.* **63**(2), 1062–1070 (2016).
- [30] E. Sariyildiz, R. Oboe, and K. Ohnishi, "Disturbance observer-based robust control and its applications: 35th anniversary overview," *IEEE Trans. Ind. Electron.* **67**(3), 2042–2053 (2020).
- [31] D. Sun, F. Naghdy, and H. Du, "Neural network based passivity control of teleoperation system under time-varying delays," *IEEE Trans. Cybern.* **47**(7), 1666–1680 (2017).
- [32] Z. Chen, F. Huang, W. Sun, J. Gu, and B. Yao, "RBF-neural-network-based adaptive robust control for nonlinear bilateral teleoperation manipulators with uncertainty and time delay," *IEEE/ASME Trans. Mechatron.* **25**(2), 906–918 (2020).
- [33] Z. Chen, F. Huang, W. Chen, J. Zhang, W. Sun, J. Chen, J. Gu, and S. Zhu, "RBFNN-based adaptive sliding mode control design for delayed nonlinear multilateral telerobotic system with cooperative manipulation," *IEEE Trans. Industr. Inform.* **16**(2), 1236–1247 (2020).
- [34] Z. Li and Y. Xia, "Adaptive neural network control of bilateral teleoperation with unsymmetrical stochastic delays and unmodeled dynamics," *Int. J. Robust Nonlinear Control.* **24**(11), 1628–1652 (2014).
- [35] X. Yang, C.-C. Hua, J. Yan, and X.-P. Guan, "A new master-slave torque design for teleoperation system by T-S fuzzy approach," *IEEE Trans. Control Syst. Technol.* **23**(4), 1611–1619 (2015).
- [36] D. Sun, Q. Liao, T. Stoyanov, et al. "Bilateral telerobotic system using Type-2 fuzzy neural network based moving horizon estimation force observer for enhancement of environmental force compliance and human perception," *Automatica* **106**, 358–373 (2019).
- [37] Z. Chen, F. Huang, C. Yang, and B. Yao, "Adaptive fuzzy backstepping control for stable nonlinear bilateral teleoperation manipulators with enhanced transparency performance," *IEEE Trans. Industr. Electron.* **67**(1), 746–756 (2020).

- [38] D. Tian, B. Zhang, H. Shen, and J. Li. “Stability Problem of Wave Variable Based Bilateral Control: Influence of the Force Source Design,” *Math. Probl. Eng.* 2013, (2013).
- [39] D. A. Lawrence, “Stability and transparency in bilateral teleoperation,” *IEEE Trans. Robot Autom.* **9**(5), 624–637 (1993).
- [40] Y. Yokokohji and T. Yoshikawa, “Bilateral control for master-slave manipulators for ideal kinesthetic coupling-formulation and experiment,” *IEEE Trans. Robot. Autom.* **10**(5), 605–620 (1994).
- [41] B. Hannaford, “A design framework for teleoperators with kinesthetic feedback,” *IEEE Trans. Robot. Autom.* **5**(4), 426–434 (1989).
- [42] B. Willaert, D. Reynaerts, and H. V. Brussel, “Bilateral teleoperation: Quantifying the requirements for and restrictions of ideal transparency,” *IEEE Trans. Control Syst. Technol.* **22**(1), 387–395 (2014).
- [43] Z. Chen, F. Huang, W. Sun, and W. Song, “An improved wave-variable based four-channel control design in bilateral teleoperation system for time-delay compensation,” *IEEE Access* **6**, 12848–12857 (2018).
- [44] A. Ramasubramanian, and L. E. Ray, “Comparison of EKF-based and classical friction compensation,” *J. Dyn. Syst. Meas. Control* **129**, 236–242 (2006).
- [45] G. J. Bierman, “Measurement Updating Using the U—D Factorization,” *Proc. IEEE Conf. Dec. Control*, pp. 337–346, (1975).
- [46] R. Gourdeau, “Adaptive Control of Robotic Manipulators,” *Ph.D. thesis, Carleton University, Canada*, (1990).
- [47] J. Craig, P. Hsu, and S. Sastry, “Adaptive Control of Mechanical Manipulators,” *Int. J. Robot. Res.* **6**(2), 16–28 (1987).
- [48] L. Chan, F. Naghdy, and D. Stirling, “An Improved Extended Active Observer for Adaptive Control of A n -DOF Robot Manipulator,” *J. Intell. Robot. Syst.* **85**(3), 679–692 (2017).